VOLUME 98 ▪ MAY/JUNE 2022

Photochemistry and Photobiology

PUBLISHED BY
THE AMERICAN SOCIETY FOR PHOTOBIOLOGY
www.wileyonlinelibrary.com/journal/php

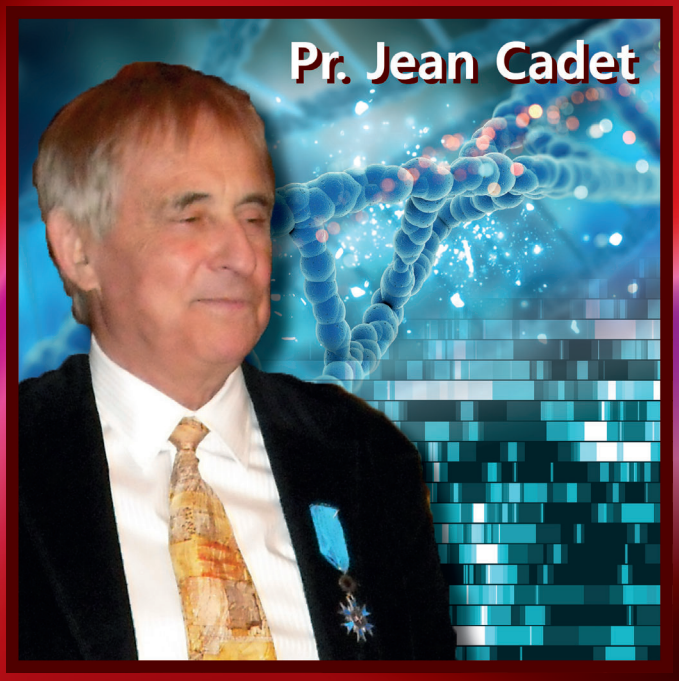

This is a Special Issue celebrating the achievements of Prof. Jean Cadet

WILEY

Photochemistry and Photobiology

The official journal of the American Society for Photobiology

PHOTOCHEMISTRY AND PHOTOBIOLOGY (ISSN: 0031-8655 [print]; ISSN: 1751-1097 [online]) is published bi-monthly on behalf of the American Society for Photobiology by Wiley Periodicals LLC, 111 River St., Hoboken, NJ 07030-5774 USA.

Periodicals Postage Paid at Hoboken, NJ and additional offices.

Postmaster: Send all address changes to *PHOTOCHEMISTRY AND PHOTOBIOLOGY*, Wiley Periodicals LLC, C/O The Sheridan Press, PO Box 465, Hanover, PA 17331 USA.

Information for subscribers: *Photochemistry and Photobiology* is published in six issues per year. Institutional subscription prices for 2022 are:

Print & Online: US$1718 (The Americas), US$1865 (Rest of World), €1211 (Europe), £955 (UK). Prices are exclusive of tax. Asia-Pacific GST, Canadian GST/HST and European VAT will be applied at the appropriate rates. For more information on current tax rates, please go to https://onlinelibrary.wiley.com/library-info/products/price-lists/payment. The price includes online access to the current and all online back files to January 1st 2017, where available. For other pricing options, including access information and terms and conditions, please visit https://onlinelibrary.wiley.com/library-info/products/price-lists. Terms of use can be found here: https://onlinelibrary.wiley.com/terms-and-conditions.

Delivery Terms and Legal Title: Where the subscription price includes print issues and delivery is to the recipient's address, delivery terms are Delivered at Place (DAP); the recipient is responsible for paying any import duty or taxes. Title to all issues transfers Free of Board (FOB) our shipping point, freight prepaid.

Claims for Missing or Damaged Print Issues

Our policy is to replace missing or damaged copies within our reasonable discretion, subject to print issue availability, and subject to the following terms: Title to all issues transfers Freight on Board ("FOB") to the address specified in the order; (1) Freight costs are prepaid by Wiley; and (2) Claims for missing or damaged copies must be submitted by the Customer or Subscription Agent within the claims window, as noted below.

Claims window - General

Claims for missing print issues must be sent to cs-agency@wiley.com (and the Subscription Agent or Customer may be referred to a society) within three months of whichever of these dates is the most recent: date of submission; or date of issue publication.

Claims window - India

Both Subscription Agents and Customers in India have 48 hours after receipt of goods to confirm that all content listed on the packing label has been received. In the event of any discrepancy, SPUR Infosolutions, Wiley's delivery partner in India, needs to be notified within forty-eight (48) hours using this email address: support@spurinfo.com. All claims will be checked against SPUR Infosolutions delivery records before the claim is accepted. The above terms for Wiley's claims policy otherwise apply.

Membership: Access to *Photochemistry and Photobiology* is included with paid membership to the American Society for Photobiology. Contact the society at www.photobiology.org for further details.

Back Issues: Single issues from current and recent volumes are available at the current single issue price from cs-journals@wiley.com. Earlier issues may be obtained from Periodicals Service Company, 351 Fairview Avenue – Ste 300, Hudson, NY 12534, USA. Tel: +1 518 822-9300, Fax: +1 518 822-9305, Email: psc@periodicals.com

PUBLISHER: *Photochemistry and Photobiology* is published by Wiley Periodicals LLC, 350 Main St., Malden, MA 02148-5020.

Journal Customer Services: For ordering information, claims and any enquiry concerning your journal subscription please go to https://wolsupport.wiley.com/s/contactsupport?tabset-a7d10=2 or contact your nearest office.
Americas: Email: cs-journals@wiley.com; Tel: +1 877 762 2974.
Europe, Middle East and Africa: Email: cs-journals@wiley.com; Tel: +44 (0) 1865 778315; 0800 1800 536 (Germany)
Asia Pacific: Email: cs-journals@wiley.com; Tel: +65 6511 8000.
Japan: For Japanese speaking support, Email: cs-japan@wiley.com.
Visit our Online Customer Help at https://wolsupport.wiley.com/s/contactsupport?tabset-a7d10=2

Production Editor: Bharathi Krishnaswamy Ramachandran (email: php@wiley.com)

Advertising: corporatesalesusa@wiley.com

View this journal online at www.wileyonlinelibrary.com/journal/php

Printed in Singapore by C.O.S. Printers Pte Ltd.

Aims and Scope: *Photochemistry and Photobiology* publishes original research articles and reviews on current topics in photoscience. Topics span from the primary interaction of light with molecules, cells, and tissue to the subsequent biological responses, representing disciplinary and interdisciplinary research in the fields of chemistry, physics, biology, and medicine.
Photochemistry and Photobiology is the official journal of the American Society for Photobiology.

Abstracting and Indexing Services: The Journal is indexed by MEDLINE, Science Citation Index, and SCOPUS. For a complete list of abstracting & indexing services, please visit www.wileyonlinelibrary.com/journal/php.

Photochemistry and Photobiology accepts articles for Open Access publication. Please visit https://authorservices.wiley.com/author-resources/Journal-Authors/open-access/hybrid-open-access.html for further information about Open Access.

Wiley is a founding member of the UN-backed HINARI, AGORA, and OARE initiatives. They are now collectively known as Research4Life, making online scientific content available free or at nominal cost to researchers in developing countries. Please visit Wiley's Content Access – Corporate Citizenship site: http://www.wiley.com/WileyCDA/Section/id-390082.html

Wiley's Corporate Citizenship initiative seeks to address the environmental, social, economic, and ethical challenges faced in our business and which are important to our diverse stakeholder groups. Since launching the initiative, we have focused on sharing our content with those in need, enhancing community philanthropy, reducing our carbon impact, creating global guidelines and best practices for paper use, establishing a vendor code of ethics, and engaging our colleagues and other stakeholders in our efforts. Follow our progress at www.wiley.com/go/citizenship

ISSN: 0031-8655 (Print)
ISSN: 1751-1097 (Online)

For submission instructions, subscription and all other information visit: www.wileyonlinelibrary.com/journal/php

Photochemistry and Photobiology

The official journal of the American Society for Photobiology • Volume 98 • No. 3 • May/June 2022

Cover Figure Caption

In this special issue, we underline the contributions, achievements, and participation in various scientific activities of Pr. Jean Cadet. He has contributed to the structural characterization of photo-induced DNA modifications leading to a greater understanding of their consequences in toxicology, DNA repair and mutagenesis. Major advances have been made by Jean and his collaborators around the world in analyzing and delineating biological implications of UV-induced photodimers, understanding mechanisms of free radical mediated oxidation of nucleic acids, in particular the reaction of singlet oxygen with biomolecules, constructing models of nucleoside modifications in oligonucleotides, and resolving dilemmas associated with artifactual oxidation in the analysis of DNA damage.This volume is a collection of 19 original and review articles. About half of the articles address the formation and repair of pyrimidine dimers, the major mutagenic type of DNA damage induced by UV and sunlight. The second compilation of articles may be grouped under the topic of photosensitization and photoionization reactions of biological targets (DNA, protein, and lipids). The photo of Jean on the front cover was taken in 2008 at the Senate in Paris, when Jean was decorated with the National Order of Merit (l'Ordre National du Mérite) by Pr. Joliot-Curie.
Photo Credit: Freepik : @kjpargeter / @GarryKillian

Photochemistry and Photobiology, 2022, 98: 662–670

Special Issue Research Article

Interstrand Crosslinking Involving Guanine: A New Major UVC Laser-Induced Biphotonic Oxidatively Generated DNA Damage†

Dimitar Angelov[1,2]*, Imtiaz Nisar Lone[2], Hervé Menoni[3] and Jean Cadet[4]*

[1]Ecole Normale Supérieure de Lyon, CNRS, Laboratoire de Biologie et de Modélisation de la Cellule LBMC, Université de Lyon, Lyon, France
[2]Izmir Biomedicine and Genome Center IBG, Dokuz Eylul University Health Campus, Balçova, Izmir, Turkey
[3]CNRS UMR 5309, INSERM U1209, Institute for Advanced Biosciences IAB, Université Grenoble Alpes, La Tronche, France
[4]Département de Médecine nucléaire et Radiobiologie, Faculté de Médecine, Université de Sherbrooke, Sherbrooke, QC, Canada

Received 17 October 2021, accepted 29 November 2021, DOI: 10.1111/php.13587

ABSTRACT

Several classes of oxidatively generated DNA damage including oxidized purine and pyrimidine bases, interstrand base crosslinks and DNA-protein crosslinks have been previously shown to be generated in both isolated DNA and cellular DNA upon exposure to either 266-nm laser irradiation or one-electron oxidants. In this study, we provide evidence that biphotonic ionization of guanine bases by UVC laser irradiation of double-stranded deoxyoligonucleotides in aerated aqueous solutions induces the formation of interstrand crosslinks (ICLs). This is supported by various experiments including sequencing gel analyses of formed photoproducts and effects of UVC laser intensity on their formation. This constitutes a novel example of the diversity of reactions of guanine radical cation that can be generated by various one-electron oxidants including UVC laser biphotonic ionization, direct effect of ionization radiation and type I photosensitizers. However, the exact structure of the interstrand base adducts that is a challenging analytical issue remains to be further established. Examples of relevant biochemical/structural applications of biphotonic induction of ICLs in DNA samples by high-intensity UVC laser pulses are provided.

INTRODUCTION

Cellular DNA is subject to a wide variety of endogenously and environmentally induced modifications including base/sugar oxidation, hydrolytic deamination and base release (1–4) together with the formation of interstrand crosslinks (ICLs) and DNA-protein adducts (5–9). ICLs that covalently link the two complementary DNA strands together constitute a serious problem to the cell because they prevent DNA strand separation and thus interfere with DNA transcription and replication. Several classes of ICLs have been characterized in model studies and also detected in the cells. For example, it has been shown that hydroxyl radical (•OH)-mediated oxidation of the 2-deoxyribose at C4' leads to the generation of a highly reactive α,ß-unsaturated keto-aldehyde intermediate that efficiently covalently adds to either cytosine (10) or adenine (11) on the opposite DNA strand. The resulting slow forming ICLs that involve cytosine have been detected in cellular DNA exposed to either gamma rays or bleomycin (12). Also, C1' abasic sites that are intermediates of the base excision repair of oxidized and alkylated bases have shown their ability to create ICLs (13). Furthermore, endogenous oxidation of lipids produces unsaturated aldehydes such as acrolein, crotonaldehyde or 4-hydroxynonenal that act as bifunctional alkylating agents, thus crosslinking guanine residues in DNA (14,15). Acetaldehyde and malonaldehyde, two endogenously formed highly reactive aldehydes, are also efficient ICL agents (7). In addition, several classes of chemical drugs including nitrogen mustards, platinums and activatable mytomycins also have the capability of generating deleterious ICLs (8). UVA irradiation of DNA in the presence of intercalating bifunctional psoralen derivatives including 8-methoxypsoralen, 5-methoxypsoralen and 4,5′,8-trimethylpsoralen (16–18) leads to the formation of ICLs that present a real challenge for DNA repair machinery (19). Poorly reactive octahedral Pt (IV) anticancer complexes have also been shown to generate thymine-Pt-guanine crosslinks upon blue light irradiation (20). Exposure of DNA to high intensity 266-nm laser pulses triggers the formation of specific photolesions including predominant oxidized bases (21,22) together with DNA-protein crosslinks (DPCs) (23,24) and minor GT intrastrand lesions (25), as the result of biphotonic ionization of the nucleobases. Interestingly, under these conditions of irradiation, DNA ICLs are also formed with an enhanced quantum yield by almost one order of magnitude with respect to the conventional UVC lamp irradiation (for a review, see (26)). This study focuses on the formation and partial characterization of ICLs in aerated aqueous solutions of DNA duplexes consisting of 20-mer deoxyoligonucleotides following exposure to high intensity 266-nm laser pulses.

*Corresponding authors email: dimitar.anguelov@ens-lyon.fr (Dimitar Angelov) and Jean.Cadet@USherbrooke.ca (Jean Cadet)
†This article is part of a Special Issue celebrating the achievements of Prof. Jean Cadet.

MATERIALS AND METHODS

Oligonucleotides. 20-mer duplex oligonucleotides A: ACATTATACGAATATTTAGA and its complementary strand B: TCTAAATATTCGTATAATGT, the mutated 20-mer A′ and B′ were the 3′-side Gs were replaced by T and A, respectively (see Figure S1), and junction oligonucleotides 1: TCACATACGCTTTGCTAGGACATC TTGATATC; 2: TGATATCAAGATGTCCATCTGTCCGTTCATC; 3: AGATGAACGGACAGATCATGGTGCTTTTAAAG; 4: TCTTTAAAA GCACCATGTAGCAAAGCGTATGTG were purchased from Eurofins and gel purified. Typically, 10 pmol of the selected oligonucleotide was 5'-end labeled by standard protocols using 20 μCi of [γ-^{32}P] ATP (Amersham) in the presence of T4 polynucleotide kinase (New England Biolab). The specific activity of the labeled probe was 2–3 × 10^6 cpm $pmol^{-1}$. Duplex DNAs were assembled by mixing an equimolar amount of the labeled and unlabeled strands in TE buffer containing 20 mM of NaCl, and after brief heating at 75°C, allowed to cool down slowly to room temperature. Four-way junctions (4WJs) were assembled as follows: 5 pmol of the [^{32}P]-labeled oligonucleotide was mixed in 10 mM of Tris-HCl, pH 8.0, 1 mM of EDTA and 100 mM of NaCl with 10 pmol of the three remaining cold oligonucleotides in a final volume of 50 μL. The mix was heated at 80°C for 3 min and left to cool down slowly to room temperature. The formation of the duplex DNA and 4WJ were tested by native PAGE.

Laser irradiation. The samples (usually 20 μL) were UV-irradiated in siliconized 0.65-mL Eppendorf tubes with a single pulse (or multiple pulses where indicated) provided from the fourth harmonic (λ = 266 nm, τ_p = 5 ns) of a Surelite II Nd:YAG laser (Continuum, Santa Clara, CA) nanosecond Nd-YAG laser. The diameter of the laser beam was adjusted to 2.8 mm to fit with the sample surface using a circular diaphragm. The pulse energy of UVC radiation was measured with a calibrated pyroelectrical detector (Ophir Optronics Ltd., Jerusalem, Israel) using an 8% deviation beam splitter. The maximum pulse irradiation dose (the pulse energy divided by the beam surface) in usual single-pulse experiments was below 0.15 J cm^{-2} in order to fulfill the "single hit" experimental conditions. Variation of the laser energy was achieved by varying the flash lamp voltage or tuning the angle of the 4th harmonic generation crystal.

In temperature dependence experiments (Fig. 4), A/B*DNA samples were irradiated at different temperatures, as indicated in Fig. 4, using a homemade PC-automated Peltier-based device synchronized with the laser source. Eppendorf tubes containing 20-μL samples were automatically positioned on the axis of the laser beam (±50 microns precision) by a stepper motor rotating mechanism and irradiated by a single 0.14 J cm^{-2} UV laser pulse after equilibration for one min at each temperature. After irradiation was completed, the samples were lyophilized and the content run on 15% sequencing PAGE.

Denaturing gel electrophoresis analysis. As illustrated in Fig. 2A, after UVC laser irradiation, DNA samples were treated either chemically with 1 M of piperidine for 30 min at 90°C or enzymatically with a mix of 0.1 units of 6-dihydroxy-5*N*-formamidopyrimidine DNA glycosylase (Fpg) and T4 endonuclease V (endo V) or with a 0.5 units of T4 DNA polymerase possessing 3′-5′ exonuclease activity (from New England Biolab). Lyophilized and treated samples together with nontreated control were re-suspended in 4 μL of formamide loading buffer and run on a 15% acrylamide:bisacrylamide 19:1 gel containing 8 M of urea and 1xTBE buffer. For experiments reported in Fig. 1, low-resolution gels l = 14 cm were used, while high-resolution (l = 40 cm) sequencing gels were used in experiments reported in Figs. 3–5. The gels were dried and exposed overnight on a Phosphor-Imager screen before scanning and subsequent quantification by a Molecular Dynamics Phosphorimager. The quantum efficiency (Q) of a lesion at an individual base (27) is defined as $Q = R/\sigma E R_0$, where R/R_0 is the ratio between the amount of the radioactivity (R) in the respective band and the total radioactivity (R_0) loaded within the lane, E is the dose of irradiation (expressed in photons per square centimeter) and σ is the absorption cross-section (σ = 2.3 10^{-17} cm^2) of DNA at 266 nm. R_0 and R were determined by volume integration using the Image Quant Software (Molecular Dynamics). The typical reproducibility of Q determined from several independent experiments was usually ~95%.

RuvA-4WJ-four-way junction experiments. Escherichia coli RuvA (RuvAEcoli) and *Mycobacterium leprae* RuvA (RuvAMle) proteins), a kind gift from Dr. Irina Tsaneva (University College London), were expressed in the *E. coli* system and purified to homogeneity as described in (28) and (29), respectively. Binding reactions with 30 fmol junction and 250 nM of RuvAEcoli and RuvAMle (sufficient to achieve full 4WJ binding as probed by control EMSA) were carried out in 10 mM of Tris pH 7.4, 1 mM of EDTA, 1 mM of DTT, 5% glycerol, 50 μg ml^{-1} of BSA. After irradiation with a single 0.15 J cm^{-2} pulse, DNA was extracted by the phenol–chloroform procedure followed by ethanol precipitated and then run on a 15% sequencing PAGE as described above.

RESULTS AND DISCUSSION

High-intensity UV laser photolysis induces formation of interstrand DNA–DNA crosslinks at guanine residues

We have shown in early studies that guanines are the primary target for one-electron oxidation of DNA in terms of final degradation products, which is achieved by a high intensity 266-nm UV laser pulse through a biphotonic ionization process (21,22). This generates purine and pyrimidine nucleobase radical cations with similar efficiency, which evolve by hole transport processes dependent on the helicoidal base stacking and pairing (30,31). Holes are preferentially trapped by guanines due to their lowest oxidation potential among DNA bases (32). As shown from detailed mechanistic studies, the main chemical reactions of the DNA base radical cations in either aqueous solutions or cells have been rationalized in terms of two main competitive pathways. Thus, hydration of predominant guanine radical cation ($Gua^{\bullet+}$) gives rise to transient 8-hydoxy-7,8-dihydroguanyl radical (33,34) that is subsequently converted into 8-oxo-7,8-dihydroguanine (8-oxoGua) and 2,4-diamino-4-hydroxy-5-formamidopyrimidine (FapyGua) by one-electron oxidation and one-electron reduction, respectively (35,36). Relatively minor competitive deprotonation of $Gua^{\bullet+}$ generates the highly oxidizing oxyl-type radical ((Gua)-H$^{\bullet}$) in dynamic equilibrium with several tautomers, that upon addition of the superoxide anion radical (37) leads to the formation of 2,2,4-triamino-5(2*H*)-oxazolone (Oz) (38), a piperidine labile compound (39,40) as FapyGua, that is however more stable (41). In addition, several relatively minor oxidation products of thymine, cytosine and adenine are also formed due to hydration/deprotonation of related radical cations (36).

Formation and chemical properties of ICLs formed in DNA duplexes

Besides the formation of the major guanine lesions, we observed in several experiments that laser irradiation of uniquely end-labeled DNA fragments resulted in additional bands migrating slower than the full-length labeled oligonucleotide during electrophoresis. To study the origin of these bands, 20-bp DNA fragments, uniquely 5′-labeled at either the top (A*/B) or the bottom (A/B*) strand, were submitted to a single dose of 0.14 J cm^{-2} or multiple laser pulses of different intensity, keeping the total irradiation dose equal to 0.14 J cm^{-2} and run on a denaturing urea-PAGE. Two strong retardation bands X1 and X2 are observed together with some less intense discrete bands and a smear (Fig. 1A), in addition to some nonspecific cleavage present in the ladder sequence. The positions and the relative intensities of the slower migrating bands are quite similar for each of the end-labeled DNAs. Quantification of overall relative radioactivity in the slow migration ladder, the full length and the fast migrating ladder is 16%, 75% and 9%, respectively, for each

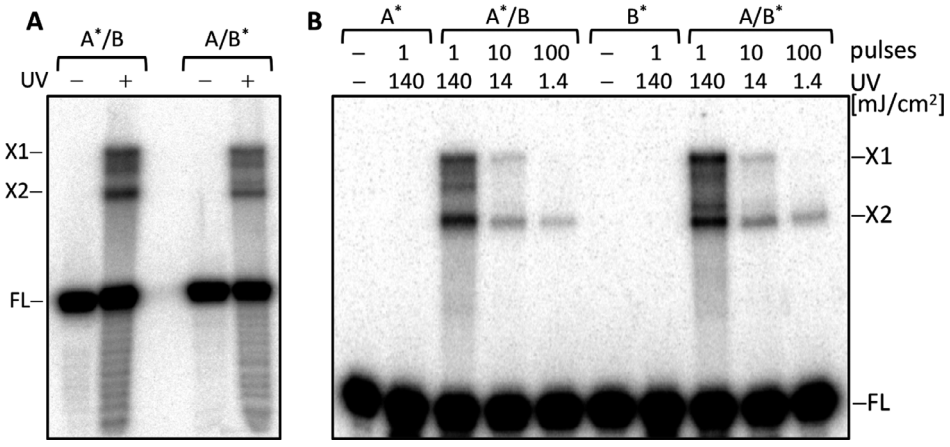

Figure 1. High-intensity UV laser pulses induce interstrand DNA crosslinking by a biphotonic absorption mechanism. (A) Denaturing gel electrophoresis pattern of a single 266 nm laser pulse-irradiated 20-mer duplex with either top A*/B or bottom A/B* strand labeled. (B) The same DNA duplexes were UV-irradiated with one or several pulses with a different laser fluence to the same total irradiation dose of 140 mJ cm^{-2}.

labeled strand. Analysis of the single-strand breaks within the fast migration ladder was already provided (22); here, we focus on the nature of the retardation bands.

Upon decreasing the laser intensity, while keeping the total irradiation dose constant by varying the number of pulses, the yield of all observed lesions decreases, thus demonstrating their biphotonic origin (Fig. 1B). However, a small fraction (10–15%) of the fast migration X2 retardation band that is still present at the lowest intensity has obviously a monophotonic origin. Interestingly, these retardation bands are absent in nonannealed but irradiated oligonucleotides A* and B* (Fig. 1B). This observation, together with the larger molecular weight of the slow-migrating DNAs, clearly demonstrates that they are formed by DNA interstrand adducts. Note that, in denaturing gels, the rate of migration of linear oligonucleotide is determined primarily by mass, while the migration of interstrand covalent adducts is determined by DNA shape, which in turn is dictated by the location of the crosslink. The presence of the two strong non-co-migrating bands might be attributed to two specifically crosslinked locations, while the weaker bands and the smear to a non-specific random crosslinking.

To identify the bases involved in the specific DNA–DNA crosslinking, one picomole (~2.10^6 cpm) of single-end labeled DNA fragments were submitted to a 0.14 J cm^{-2} laser pulse, lyophilized and run on denaturing PAGE. The bands corresponding to the full length 20-mer oligonucleotide and the two retardation bands were excised from the gel, and eluted DNA fragments were treated as indicated in Fig. 2, prior to sequencing PAGE analysis (Fig. 3). Piperidine treatment was used to probe the formation of oxazolone (Oz) and FapyGua, two of the main laser-induced oxidatively generated DNA lesions; ICLs were also shown to be piperidine-labile. The mix of Fpg glycosylase and T4 endonuclease V (endo V) was used to probe 8-oxoGua, the other main oxidation lesion, and also monophotonic cyclobutane pyrimidine dimers (CPDs), respectively. The T4 DNA polymerase digestion was performed to probe all DNA lesions that constitute full or partial stops for its 3′ to 5′ exonuclease activity, essentially pyrimidine dimers and interstrand crosslinks.

The nontreated crosslinked X1 samples for both strands (Fig. 3A,B lanes 3) shows a weak gel-condition lability at the centrally located guanine liberating a free 3′-OH termini

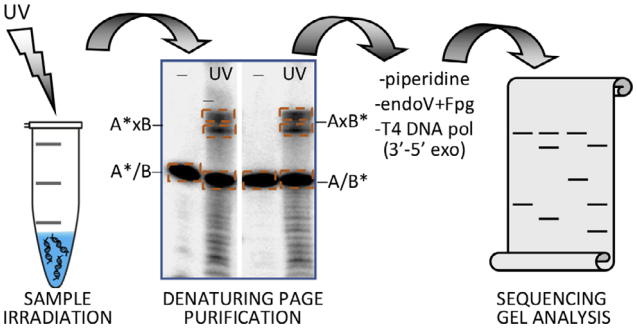

Figure 2. Protocol used for mapping the UV laser-induced DNA lesions: oxazolone (Oz) and crosslinks (piperidine); 8-oxoGua (Fpg glycosylase) cyclobutane pyrimidine dimers (CPDs) (T4 endonuclease V); (CPDs, crosslinks (T4 DNA polymerase)). The denaturing PAGE image shown in the figure is the original preparative gel used for gel elution purification of the different species as indicated by rectangles.

fragment, together with a slightly more stronger elimination of the crosslinks releasing some small amount of full-length (FL) oligonucleotides (Fig. 3A,B lanes 3,4).

Under the combined Fpg glycosylase and endo V treatment of the gel purified irradiated A*-labeled species, the 8-oxoGua bands at the central guanine and CPDs at the 3′-side TTT run present in the treated fraction of FL (lane 6A) disappear in X1 species (lane 7A), while their intensity is reduced by twice in the X2 species (lane 8A) with respect to the FL oligonucleotide (lane 6A). These observations strongly suggest that slow migrating adducts A*xB-X1 (lane 7A) involve central guanine(s), while faster migrating adducts (lane 8A) involve oligonucleotide ends. Note that 8-oxoGua related to the middle guanine in the bottom strand labeled 20-mers A/B* is poorly generated (Fig. 3B lanes 6–8), thus precluding the possibility of similar analysis for this strand to be performed.

Hot piperidine treatment (Fig. 3A,B, lanes 10–12) confirms these suggestions and provides additional information on some properties of the ICLs. Rapid inspection of the electrophoresis patterns shows that crosslinked adducts are partially piperidine labile resulting in central guanines (lane 11A,B) and full-length cleavage fragments (lanes 11A,B and 12A,B). The central and the 3'-proximal piperidine labile bands at guanines represent

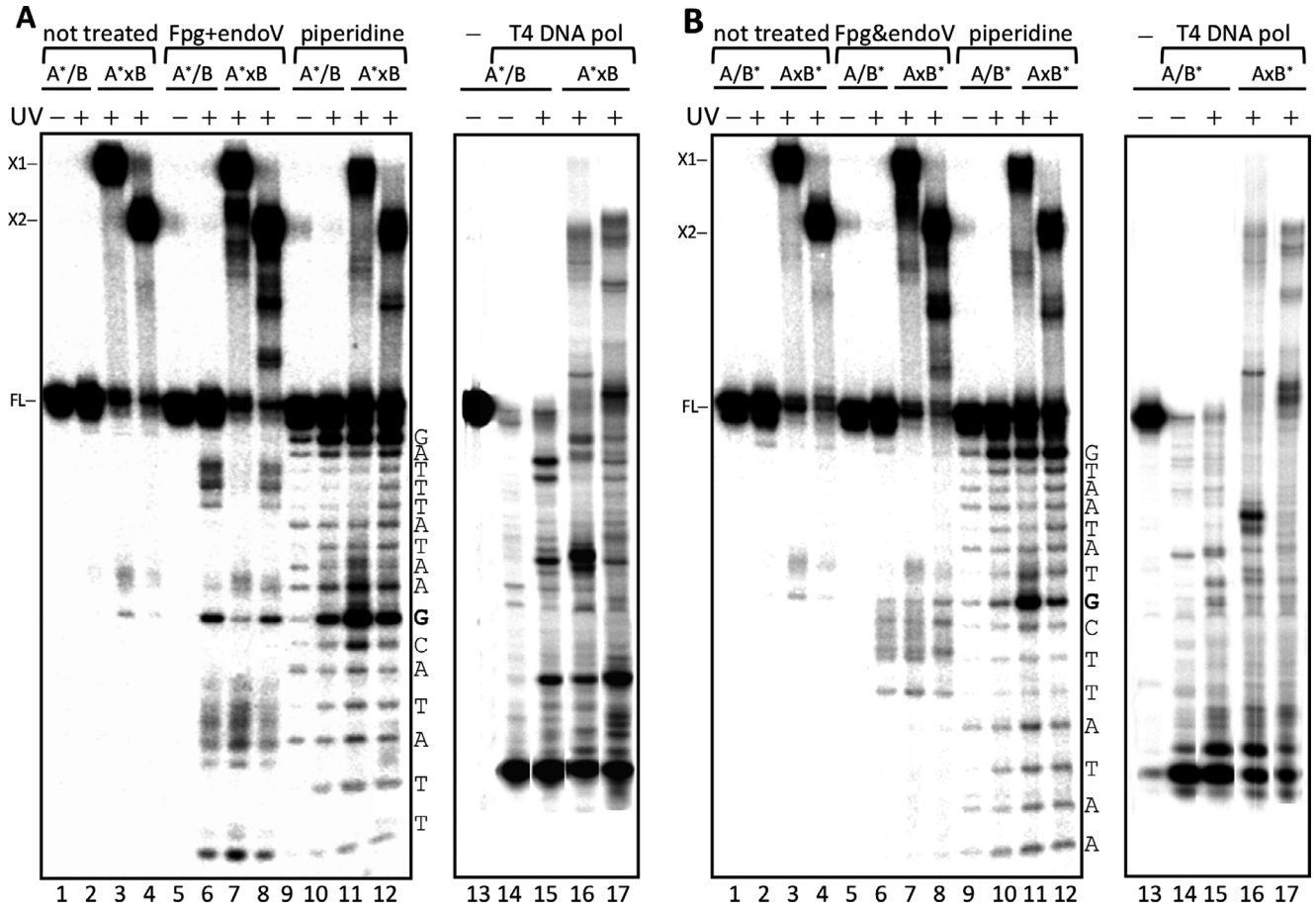

Figure 3. DNA ICLs are located at guanines. Sequencing gel analysis of DNA–DNA crosslinks using gel purified species as illustrated in Fig. 2 and treated as indicated. A*/B top strand labeled duplex (A). A/B*: bottom strand labeled duplex (B). A*xB (AxB*) top (bottom) crosslinked DNA–DNA adducts. Lanes 3,7,16 correspond to the X1, lanes 4,8,17 to the X2 and lines 1,2,5,6,8,9 to the FL gel purified samples. Note that hot piperidine treatment and Fpg protein-catalyzed excision reaction releases ^{32}P-5′-fragment with free 3′-OH termini which migrate as Maxam–Gilbert fragments. In contrast, endo V and T4 DNA polymerase released ^{32}P-5′-fragments migrate 1 to 2.5 nucleotides slower.

most likely cleaved oxidized guanine bases (Oz, FapyGua) and crosslinked residues. While the intensities of the central guanine bands for the FL oligonucleotides (lane 10A,B) are similar with the respective intensities for the X2 species (lanes 12A,B), the intensities of the X1 species are considerably higher. This confirms the central guanine assignment of the slowly migrating crosslinked species X1. At the same time, the equal intensity at the 3'-proximal guanine bands in all 3 lanes 10A,B-12A,B suggests that they belong solely to oxazolone (Oz) and FapyGua lesions, and that this guanine precursor is not involved in crosslinking. Otherwise, we would observe an enhancement of the 3′ piperidine-induced cleavage at this guanine in lanes 12A,B if crosslinked. This raises the question whether end-positioned crosslinks involve the 3′-proximal guanines or originate from specific border effects. To test this possibility, we performed the same crosslinking experiments as in Fig. 1 but with 20 bp DNA duplexes A′/B′, where the 3′-proximal G/C base pairs in the upper and lower strands were replaced by T/A and A/T, respectively. Interestingly, this substitution of the two 3′-proximal guanines did not result in any qualitative and quantitative change of the gel retardation crosslinking profiles that remained identical with that in Fig. 1 (Figure S1). The persistent fast migration band X2 in absence of the 3′-proximal guanines provides evidence that crosslinking at the DNA ends is a guanine-independent border effect. Moreover, DNA extremities crosslinking at DNA ends is occurring surprisingly under monophotonic excitation too, but with a highly reduced efficiency (low laser fluence, Fig. 1B). This is most likely a border effect arising from particular properties of DNA edges at specific traps within the charge/energy migration process (27), together with a favorable conformation to crosslinking reactivity.

This localization of the laser DNA crosslinks is further confirmed by the electrophoretic profiles of T4 DNA polymerase 3′-5′ exonuclease digestion profiles (Fig. 3A,B, lanes 14-17). Major digestion stops are observed at middle guanines and DNA end crosslinks together with stops at pyrimidine dimers, and the corresponding released 5'-labeled fragments migrate 1–2.5 nt slower than the respective Maxam-Gilbert fragments (lanes 16A, B and 17A,B). Interestingly, while exonuclease digestion stops at pyrimidine dimers known to be blocking lesions, the majority of crosslinks are bypassed by the 3′-5′ exonuclease digestion, releasing finally small undigested 5'-oligonucleotides migrating at the bottom of the gel.

Mechanisms of UVC laser-induced formation of ICLs

First, it may be ruled out that the detected ICLs would result from UV crosslinking of the complementary A/B strands as previously

observed in sequences rich in (A + T) content (42,43). As discussed in the previous section, experimental evidence is provided that guanines, essentially central guanine in X1 band, are mostly involved in the high-intensity UVC laser-mediated formation of ICLs in the 20-mer duplex oligonucleotides. The biphotonic characteristic of interstrand DNA photoaddition is strongly suggestive of the participation of the guanine radical cation ($Gua^{\bullet+}$) as the highly reactive intermediate in the generation of ICLs. It may be reminded that high intensity UVC nanosecond laser pulses are able to photo-ionize the four main pyrimidine and purine bases of isolated 2′-deoxyribonucleosides in aqueous solutions. However, a major redistribution of the base radical cations generated in either isolated DNA duplexes (21,22) or cellular DNA (25,44,45) through efficient charge transfer with preferential positive hole trapping by the guanine bases has been demonstrated. This is confirmed in this study by the predominant formation of piperidine-labile sites and Fpg-sensitive sites at guanine bases. Furthermore, abundant information is available on the reactivity of $Gua^{\bullet}$ toward several nucleophiles including hydroxide anion (33,34), N3 atom of thymine (46,25), free amino group of polylysine (47–49) and polyamines (50,51). The formation of ICL could be explained by the covalent bond formation between $Gua^{\bullet+}$ and cytosine or guanine through 4- and 2-amino group, respectively, on the opposite strand. However, identification of the ICLs requires additional structural information that may be gained from further experimental/theoretical studies.

Interstrand Crosslinks as biochemical probes of DNA conformation

Interstrand DNA–DNA crosslinks: a tool for local denaturation probing. Laser crosslinking at guanines can be used as a photoactivation probe of the fluctuational opening of individual GC base pairs and the structure of DNA itself, which are both strongly temperature-dependent. When the molecule is heated up to a sufficiently high temperature (70°C to 90°C, depending on the sequence and the salt conditions), the DNA helix is thermally denatured. The fluctuations are so large that they break all the hydrogen bonds connecting the two strands, and the strands separate from each other. Since interstrand crosslinking is a function of base pairing, we applied this approach aimed at providing a measure of the temperature-induced local DNA closing probability.

Duplex A/B* DNA aliquots were submitted to a single 0.14 J cm^{-2} laser pulse at different temperatures in 10 mM of Tris, pH 7.6 at two different salt conditions as shown in Fig. 4A,B). The upper panels of the figure represent the gel images at 20 mM of NaCl (A) and at 20 mM of NaCl, 1.5 mM of $MgCl_2$ (B), respectively. The bottom panels show the quantified data in terms of quantum efficiency of crosslinking corresponding to the two major retardation bands X1 and X2 plotted versus the temperature (Fig. 2A,B lower panels).

As can be seen from the gel images (Fig. 4, top panels), the crosslinking ladder decreases gradually as the temperature increases. The decrease is more prompt after certain temperatures and disappears completely at temperatures above 44°C (52°C, at 1.5 mM of $MgCl_2$). The shape of the quantum efficiency versus the temperature (Fig 4, bottom panels) is quite similar to that of a classical UV absorption melting curve. Interestingly, the melting temperature T_m for the magnesium-free solution ~39°C coincides with the one calculated by classic formulae value for 20 mM of NaCl and ~1 nM of DNA substrate (Fig. 4A). As expected, the addition of 1.5 mM of $MgCl_2$ leads to an important

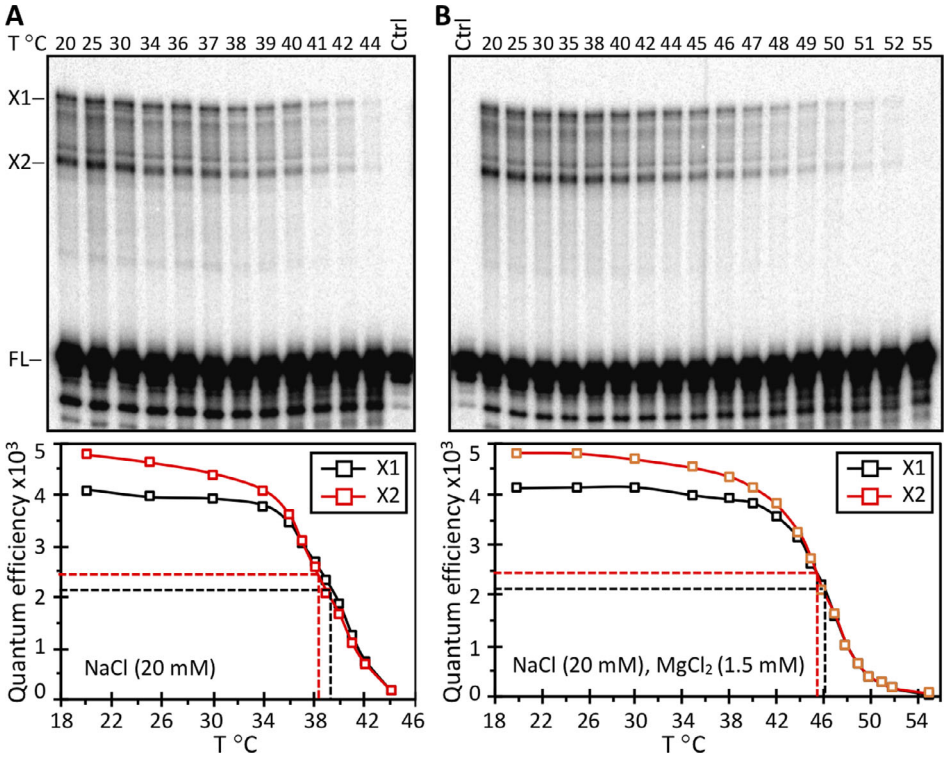

Figure 4. Temperature melting profiles of the up-shifted ladder and full-length (FL) DNA of UV laser irradiated-20 mer A/B* duplexes at different salt conditions: 20 mM of NaCl (A) and 20 mM of NaCl + 1.5 mM of $MgCl_2$ (B). Upper panels—gel images, lower panels—quantified intensities for the corresponding middle-guanines crosslinks—X1 (black rectangles) and DNA borders crosslinks—X2.

rise of T_m by ~7.0° (Fig. 4B). Importantly, T_m value at the middle guanine (X1) is ~1°C higher that Tm at the DNA extremities (X2) (~0.5°C in the presence of 1.5 mM of $MgCl_2$). This might be an indication of a slightly delayed full strand separation relative to the DNA ends opening.

This experiment shows how interstrand DNA–DNA crosslinking can be used as a direct sensor of local double helix melting in short DNA fragments, providing information on the local fluctuation opening of practically all GC base pairs in a single experiment. This has already been exploited for probing the temperature-dependent DNA "breathing" induced "denaturation bubbles" formation in natural promoter "TATA-box" containing DNA constructs with strongly "closed" extremities by multiple GC runs (52). The experimental observations provided evidence that DNA "breathing" is particularly strong in AT-rich regions that exhibited premelting character starting at close to physiological temperatures (52).

Suppression of the interstrand crosslinking at the crossover region in 4WJ DNA-RuvA complexes. Four-way junctions (4WJ) are crossover DNA intermediates that form in all organisms during homologous recombination and double-strand breaks repair. The successful completion of these processes requires resolution of the crossover by specialized proteins such as RuvABC proteins—a highly conserved and widely represented class of proteins in prokaryotes, involved in the late stage of the *E. coli* recombination process. The crystal structure of RuvA revealed the molecular basis of binding to a synthetic Holliday junction

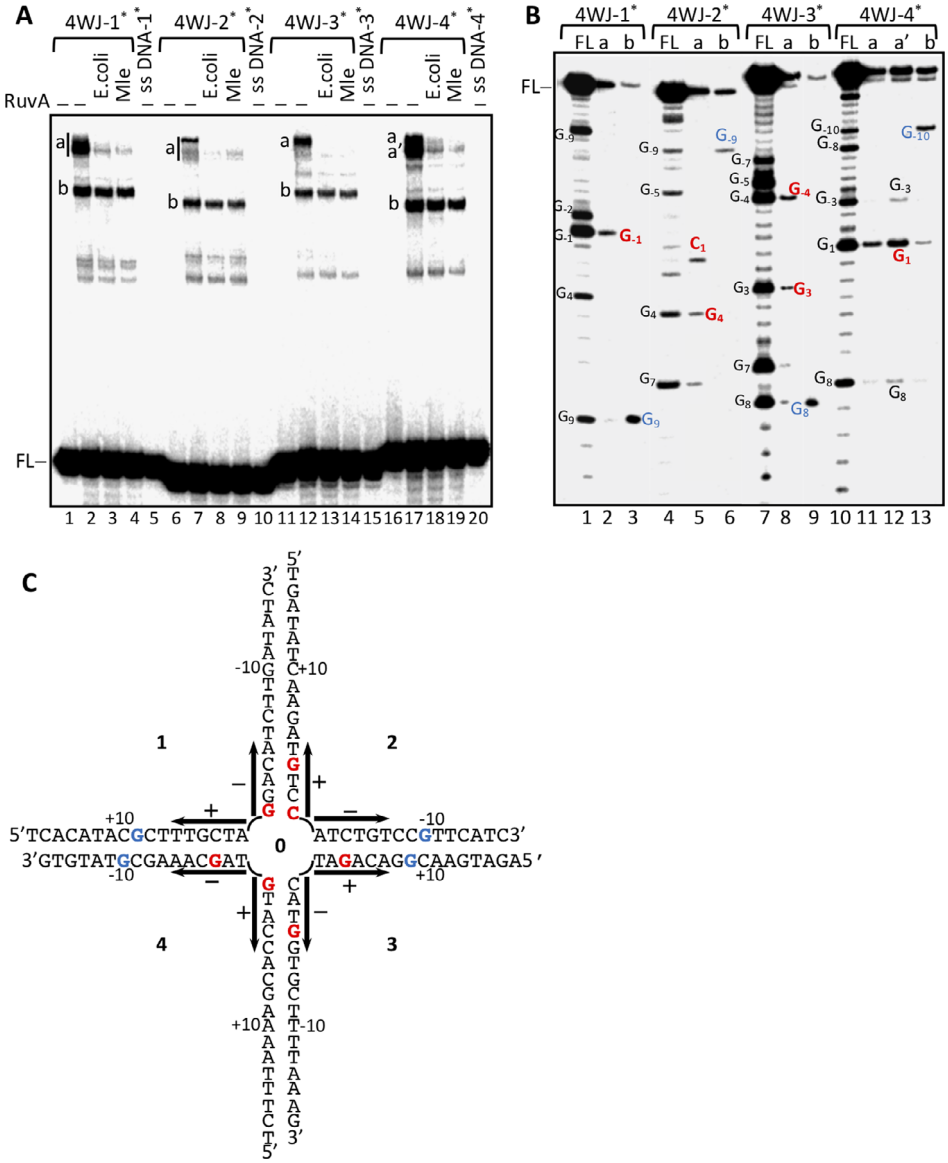

Figure 5. Sequencing PAGE analysis of the DNA–DNA crosslinking in uniquely 5′-labeled 4WJ 1*–4*, free and RuvA complexed. (A) Slow migration DNA ladder of a single 0.14 J cm^{-2} pulse irradiated free (lanes 2, 7, 12, 17) and RuvAEcoli (lanes 3, 8, 13, 18) and RuvAMle (lanes 4, 9, 14, 19) complexed junctions labeled as indicated. Lanes 1, 6, 11, 16 correspond to nonirradiated controls and lanes 5, 10, 15, 20 to irradiated single-stranded oligonucleotides 1*–4*. (B) Sequencing gel analysis after piperidine treatment of DNA–DNA crosslinks "a" and "b" and FL species isolated from the gel in A (lanes 2, 7, 12, 17). (C) Schematics of the results of mapping the crosslinked base residues within the bands "a" and "b", marked by red and blue color, respectively. Upon RuvA binding, the inhibited crosslinking residues (band "a") are in red and the nonmodified (band "b") in blue.

(53). In this complex, the junction was found to be sandwiched between two tetramers of RuvA. Interactions with both faces of DNA appeared to distort base-pairing in the arms, facilitating the disruption of base stacking and pairing around the central point of strand exchange. However, the crystal structure resolution was insufficient to firmly establish whether local strand separation is induced by the RuvA octamer directly or if its role is just to destabilize the crossover region and transmit the ATPase activity of the docked hexameric RuvB rings into DNA movement.

To probe the presence of eventual site-specific GC base pair opening preventing the formation of ICS induced by RuvA binding, we compared the sequencing gel retardation profiles of a single laser pulse irradiated free and RuvA complexed 4WJ assembled with each one the 5′-labeled strands 1*–4* (see the schematics in Fig. 5C). Experiments were carried out with purified RuvA from *E. coli* and *M. leprae* as described in the experimental section. As seen on Fig. 5A, the presence of bound RuvA completely inhibits the crosslink formation corresponding to the slowest migration bands "a," while all remaining faster migrating up-shifted bands remains unaffected. This site-specific total inhibition of the ICL formation at slow migrating band suggests a localized base pair opening. The rule established in the previous paragraph that "slower is the retardation band, closer to the center is the position of the crosslinked guanine residue" suggests that the footprinted guanines are the nearest to the 4WJ center. To firmly identify the footprinted residues, we excised the bands "a," "b" and FL from the gel lanes 2A, 7A, 12A, 17A and the eluted and piperidine-treated species were analyzed by sequencing gel (Fig. 5B). Interestingly, all the piperidine labile DNA–DNA adducts analyzed belong to guanine bases, with the exception of C_1 (line 5B). Note that the cleavage bands in lanes 1B, 4B, 7B and 10B are guanines mass markers from the FL fragments. Considering that the piperidine labile residues within the bands "a" (Fig. 5B, lanes 2, 5, 8, 11, 12) belong to the "footprinted" bands and residues within the bands "b" (Fig. 5B, lanes 3, 6, 9, 13) belong to the nonmodified guanines, we can conclude that RuvA binding prevents crosslinking formation at GC base pairs located in the vicinity of the 4WJ crossover. This RuvA-induced site-specific transition to a stable noncrosslinkable configuration strongly suggests occurrence of base pair opening at the crossover region. This observation is consistent with another crystal structure of a 4WJ-RuvA complex showing that local unstacking of bases occurs only in the vicinity of the central crossover point of the junction (54-55). Note that eventual protein-DNA crosslinks and protein-mediated electron transfer "repair" of the initial G radical cation could also partially contribute to the observed interstrand crosslinking inhibition of central guanines.

CONCLUSION

In this work, we report the occurrence of a new one-electron oxidation DNA lesion: interstrand crosslinks, under high-intensity single nanosecond UV laser pulse photolysis of short oligonucleotide duplexes. Two groups of ICLs were observed: one involving guanine residues independently of their location, and another one at the DNA ends independently on the presence of guanines at that position. These oxidatively generated DNA lesions are partially sensitive to hot piperidine treatment, resulting in either elimination of the crosslinked guanine or homolytic cleavage of the crosslink and release of the full-length oligonucleotide. The occurrence of this modification is highly sensitive to local DNA structural deformations. Examples are provided demonstrating the use of ICLs at guanines as sensors of temperature or protein-binding-induced local GC base pair opening. Laser-induced ICL formation was also used to probe *in vitro* the TRF2-assisted strand invasion with telomeric DNA sequences (56). Experiments on chemical structure determination of ICLs by means of HPLC-MS/MS and MALDI-TOF are under way. Finally, single-pulse crosslinking can be combined with either a rapid temperature jump provided by a mid-infrared nanosecond Er:YAG laser, or a stopped flow device to perform fast kinetic local melting or strand invasion experiments with a single-base resolution.

Acknowledgements—The authors thank Jean-Luc Ravanat from CEA-Grenoble for earlier contribution to ICL identification, Dr. Irina Tsaneva from University College London from providing the purified RuvA proteins and Deniz Donmez from IBG-Izmir for proofreading and editing the manuscript. This work was supported by institutional funding of IBG and benefitted from the 2247-A National Lead Researchers Program of TUBITAK (Project No: 120C149). The financial support received from TUBITAK does not mean that the content of the publication is approved in a scientific sense by TUBITAK. This work was also supported by institutional funds from CNRS, Ecole Normale Supérieure de Lyon and by the grant 235069 DyProSome from, Agence Nationale de la Recherche ANR, France

CONFLICT OF INTEREST

The authors declare no conflict of interest.

SUPPORTING INFORMATION

Additional supporting information may be found online in the Supporting Information section at the end of the article:

Figure S1. Denaturing gel electrophoresis of mutated DNA duplexes lacking the 3' guanines A′/B′ were submitted to one or several UV laser pulses with a different laser fluence to the same total irradiation dose of 140 mJ cm^{-2} and the sequence of the A′/B′ mutated DNA dupexe used.

REFERENCES

1. Lindahl, T. and B. Nyberg (1972) Rate of depurination of native deoxyribonucleic acid. *Biochemistry* **11**, 3610–3618.
2. Frederico, L. A., T. A. Kunkel and B. R. Shaw (1990) A sensitive genetic assay for the detection of cytosine deamination: Determination of rate constants and the activation energy. *Biochemistry* **29**, 2532–2537.
3. Cadet, J. (1994) DNA damage caused by oxidation, deamination, ultraviolet radiation and photoexcited psoralens. *IARC Sci. Publ* 245–276.
4. Cadet, J. and J. R. Wagner (2013) DNA Base Damage by Reactive Oxygen Species, Oxidizing Agents, and UV Radiation. *Cold Spring Harb. Perspect. Biol* **5**, a012559.
5. Cadet, J., J.-L. Ravanat, M. TavernaPorro, H. Menoni and D. Angelov (2012) Oxidatively generated complex DNA damage: Tandem and clustered lesions. *Cancer Lett* **327**, 5–15.
6. Groehler, A., A. Degner and N. Y. Tretyakova (2017) Mass spectrometry-based tools to characterize DNA-protein cross-linking by *Bis*-electrophiles. *Basic Clin. Pharmacol. Toxicol* **121**, 63–77.

7. Barnes, J. L., M. Zubair, K. John, M. C. Poirier and F. L. Martin (2018) Carcinogens and DNA damage. *Biochem. Soc. Trans* **46**, 1213–1224.
8. Rycenga, H. B. and D. T. Long (2018) The evolving role of DNA inter-strand crosslinks in chemotherapy. *Curr. Opin. Pharmacol* **41**, 20–26.
9. Housh, K., J. S. Jha, T. Haldar, S. B. M. Amin, T. Islam, A. Wallace, A. Gomina, X. Guo, C. Nel, J. W. Wyatt and K. S. Gates (2021) Formation and repair of unavoidable, endogenous interstrand cross-links in cellular DNA. *DNA Repair* **98**, 103029.
10. Regulus, P., S. Spessotto, M. Gateau, J. Cadet, A. Favier and J.-L. Ravanat (2004) Detection of new radiation-induced DNA lesions by liquid chromatography coupled to tandem mass spectrometry. *Rapid Commun. Mass Spectrom* **18**, 2223–2228.
11. Sczepanski, J. T., A. C. Jacobs, A. Majumdar and M. M. Greenberg (2009) Scope and mechanism of interstrand cross-link formation by the C4′-oxidized abasic site. *J. Am. Chem. Soc* **131**, 11132–11139.
12. Regulus, P., B. Duroux, P.-A. Bayle, A. Favier, J. Cadet and J.-L. Ravanat (2007) Oxidation of the sugar moiety of DNA by ionizing radiation or bleomycin could induce the formation of a cluster DNA lesion. *Proc. Natl. Acad. Sci* **104**, 14032–14037.
13. Housh, K., J. S. Jha, Z. Yang, T. Haldar, K. M. Johnson, J. Yin, Y. Wang and K. S. Gates (2021) Formation and repair of an interstrand DNA cross-link arising from a common endogenous lesion. *J. Am. Chem. Soc.* **143**(37), 15344–15357.
14. Kozekov, I. D., L. V. Nechev, M. S. Moseley, C. M. Harris, C. J. Rizzo, M. P. Stone and T. M. Harris (2003) DNA interchain cross-links formed by acrolein and crotonaldehyde. *J. Am. Chem. Soc* **125**, 50–61.
15. Minko, I. G., I. D. Kozekov, T. M. Harris, C. J. Rizzo, R. S. Lloyd and M. P. Stone (2009) Chemistry and biology of DNA containing 1, N^2-deoxyguanosine adducts of the α, β-unsaturated aldehydes acrolein, crotonaldehyde, and 4-hydroxynonenal. *Chem. Res. Toxicol* **22**, 759–778.
16. Hearst, J. E. (1981) Psoralen photochemistry. *Ann. Rev. Biophys. Bioeng.* **10**(1), 69–86.
17. Brulikova, L., J. Hlavac and P. Hradil (2012) DNA interstrand cross-linking agents and their chemotherapeutic potential. *Curr. Med. Chem* **19**, 364–385.
18. Baptista, M. S., J. Cadet, A. Greer and A. H. Thomas (2021) Photosensitization reactions of biomolecules: Definition, targets and mechanisms. *Photochem. Photobiol* **97**(6), 1456–1483.
19. McHugh, P. J., V. J. Spanswick and J. A. Hartley (2001) Repair of DNA interstrand crosslinks: molecular mechanisms and clinical relevance. *Lancet Oncol.* **2**, 483–490.
20. Zhang, J., W. Zeng, K. Wu, J. Ye, Y. Cheng, Y. Cheng, T. Zou, N. Peng, X. Wu, Y. Zhao and F. Wang (2020) Unexpected thymine oxidation and collision-induced thymine-Pt-guanine cross-linking on 5′-TpG and 5′-GpT by a photoactivatable diazido Pt(IV) anticancer complex. *Inorg. Chem.* **59**, 8468–8480.
21. Douki, T., J.-L. Ravanat, D. Angelov, J. R. Wagner and J. Cadet. (2004) Effects of duplex stability on charge-transfer efficiency within DNA. In *Long-range charge transfer in DNA I*, Vol. **236** (Edited by G. B. Schuster), pp. 1–25. Springer Berlin Heidelberg, Berlin, Heidelberg.
22. Angelov, D., A. Spassky, M. Berger and J. Cadet (1997) High-intensity UV laser photolysis of DNA and purine 2′-deoxyribonucleosides: Formation of 8-oxopurine damage and oligonucleotide strand cleavage as revealed by HPLC and gel electrophoresis studies. *J. Am. Chem. Soc* **119**, 11373–11380.
23. Moss, T., S. I. Dimitrov and D. Houde (1997) UV-laser crosslinking of proteins to DNA. *Methods* **11**, 225–234.
24. Angelov, D., J. M. Vitolo, V. Mutskov, S. Dimitrov and J. J. Hayes (2001) Preferential interaction of the core histone tail domains with linker DNA. *Proc. Natl. Acad. Sci* **98**, 6599–6604.
25. Madugundu, G. S., J. R. Wagner, J. Cadet, K. Kropachev, B. H. Yun, N. E. Geacintov and V. Shafirovich (2013) Generation of guanine-thymine cross-links in human cells by one-electron oxidation mechanisms. *Chem. Res. Toxicol* **26**, 1031–1033.
26. Nikogosyan, D. N. (1990) Two-quantum UV photochemistry of nucleic acids: comparison with conventional low-intensity UV photochemistry and radiation chemistry. *Int. J. Radiat. Biol* **57**, 233–299.
27. Angelov, D., B. Beylot and A. Spassky (2005) Origin of the heterogeneous distribution of the yield of guanyl radical in UV laser photolyzed DNA. *Biophys. J.* **88**, 2766–2778.
28. Tsaneva, I. R., G. Illing, R. G. Lloyd, S. C. West (1992) Purification and properties of the RuvA and RuvB proteins of Escherichia coli. *Mol. Gen. Genet. MGG* **235**, 1–10.
29. Arenas-Licea, J., A. J. van Gool, A. J. Keeley, A. Davies, S. C. West and I. R. Tsaneva (2000) Functional interactions of *Mycobacterium leprae* RuvA with *Escherichia coli* RuvB and RuvC on holliday junctions 1 1Edited by M. Yaniv. *J. Mol. Biol.* **301**, 839–850.
30. Spassky, A. and D. Angelov (1997) Influence of the local helical conformation on the guanine modifications generated from one-electron DNA oxidation. *Biochemistry* **36**, 6571–6576.
31. Douki, T., D. Angelov and J. Cadet (2001) UV laser photolysis of DNA: Effect of duplex stability on charge-transfer efficiency. *J. Am. Chem. Soc* **123**, 11360–11366.
32. H.-A. Wagenknecht (ed.) (2005) *Charge transfer in DNA: from mechanism to application*. Wiley-VCH, Weinheim.
33. Kasai, H., Z. Yamaizumi, M. Berger and J. Cadet (1992) Photosensitized formation of 7,8-dihydro-8-oxo-2'-deoxyguanosine (8-hydroxy-2'-deoxyguanosine) in DNA by riboflavin: a nonsinglet oxygen-mediated reaction. *J. Am. Chem. Soc* **114**, 9692–9694.
34. Rokhlenko, Y., J. Cadet, N. E. Geacintov and V. Shafirovich (2014) Mechanistic aspects of hydration of guanine radical cations in DNA. *J. Am. Chem. Soc* **136**, 5956–5962.
35. Steenken, S. (1989) Purine bases, nucleosides, and nucleotides: Aqueous solution redox chemistry and transformation reactions of their radical cations and e- and OH adducts. *Chem. Rev.* **89**, 503–520.
36. Cadet, J., J. R. Wagner, V. Shafirovich and N. E. Geacintov (2014) One-electron oxidation reactions of purine and pyrimidine bases in cellular DNA. *Int. J. Radiat. Biol* **90**, 423–432.
37. Misiaszek, R., C. Crean, A. Joffe, N. E. Geacintov and V. Shafirovich (2004) Oxidative DNA damage associated with combination of guanine and superoxide radicals and repair mechanisms via radical trapping. *J. Biol. Chem.* **279**, 32106–32115.
38. Cadet, J., T. Douki and J.-L. Ravanat (2008) Oxidatively generated damage to the guanine moiety of DNA: Mechanistic aspects and formation in cells. *Acc. Chem. Res* **41**, 1075–1083.
39. Kino, K., I. Saito and H. Sugiyama (1998) Product analysis of GG-specific photooxidation of DNA via electron transfer: 2-aminoimidazolone as a major guanine oxidation product. *J. Am. Chem. Soc* **120**, 7373–7374.
40. Gasparutto, D., J.-L. Ravanat, O. Gérot and J. Cadet (1998) Characterization and chemical stability of photooxidized oligonucleotides that contain 2,2-diamino-4-[(2-deoxy-β-D – *erythro*-pentofuranosyl) amino]-5(2 *H*)-oxazolone. *J. Am. Chem. Soc* **120**, 10283–10286.
41. Haraguchi, K., M. O. Delaney, C. J. Wiederholt, A. Sambandam, Z. Hantosi and M. M. Greenberg (2002) Synthesis and characterization of oligodeoxynucleotides containing formamidopyrimidine lesions and nonhydrolyzable analogues. *J. Am. Chem. Soc* **124**, 3263–3269.
42. Nejedlý, K., R. Kittner, Š. Pospíšilová and J. Kypr (2001) Crosslinking of the complementary strands of DNA by UV light: dependence on the oligonucleotide composition of the UV irradiated DNA. *Biochim. Biophys. Acta BBA – Gene Struct. Expr* **1517**, 365–375.
43. Nejedlý, K., R. Kittner and J. Kypr (2001) Genomic DNA regions whose complementary strands are prone to UV light-induced crosslinking. *Arch. Biochem. Biophys* **388**, 216–224.
44. Douki, T., J.-L. Ravanat, J.-P. Pouget, I. Testard and J. Cadet (2006) Minor contribution of direct ionization to DNA base damage induced by heavy ions. *Int. J. Radiat. Biol* **82**, 119–127.
45. Cadet, J., J. R. Wagner and D. Angelov (2019) Biphotonic ionization of DNA: From model studies to cell. *Photochem. Photobiol.* **95**, 59–72.
46. Crean, C., Y. Uvaydov, N. E. Geacintov and V. Shafirovich (2008) Oxidation of single-stranded oligonucleotides by carbonate radical anions: generating intrastrand cross-links between guanine and thymine bases separated by cytosines. *Nucleic Acids Res.* **36**, 742–755.
47. Perrier, S., J. Hau, D. Gasparutto, J. Cadet, A. Favier and J.-L. Ravanat (2006) Characterization of lysine-guanine cross-links upon one-electron oxidation of a guanine-containing oligonucleotide in the presence of a trilysine peptide. *J. Am. Chem. Soc* **128**, 5703–5710.
48. Safaeipour, M., J. Jauregui, S. Castillo, M. Bekarian, D. Esparza, M. Sanchez and E. D. A. Stemp (2019) Glutathione directly intercepts DNA radicals to inhibit oxidative DNA–protein cross-linking induced by the one-electron oxidation of guanine. *Biochemistry* **58**, 4621–4631.

49. Chan, C.-H., A. Monari, J. L. Ravanat and E. Dumont (2019) Probing interaction of a trilysine peptide with DNA underlying formation of guanine–lysine cross-links: Insights from molecular dynamics. *Phys. Chem. Chem. Phys* **21**, 23418–23424.
50. Silerme, S., L. Bobyk, M. Taverna-Porro, C. Cuier, C. Saint-Pierre and J.-L. Ravanat (2014) DNA-polyamine cross-links generated upon one electron oxidation of DNA. *Chem. Res. Toxicol.* **27**, 1011–1018.
51. Bignon, E., C.-H. Chan, C. Morell, A. Monari, J.-L. Ravanat and E. Dumont (2017) Molecular dynamics insights into polyamine-DNA binding modes: Implications for cross-link selectivity. *Chem. – Eur. J* **23**, 12845–12852.
52. Cuesta-López, S., H. Menoni, D. Angelov and M. Peyrard (2011) Guanine radical chemistry reveals the effect of thermal fluctuations in gene promoter regions. *Nucleic Acids Res.* **39**, 5276–5283.
53. Roe, S. M., T. Barlow, T. Brown, M. Oram, A. Keeley, I. R. Tsaneva and L. H. Pearl (1998) Crystal structure of an octameric RuvA–Holliday junction complex. *Mol. Cell* **2**, 361–372.
54. Rafferty, J. B., S. E. Sedelnikova, D. Hargreaves, P. J. Artymiuk, P. J. Baker, G. J. Sharples, A. A. Mahdi, R. G. Lloyd and D. W. Rice (1996) Crystal structure of DNA recombination protein RuvA and a model for its binding to the Holliday junction. *Science* **274**, 415–421.
55. Yamada, K., T. Miyata, D. Tsuchiya, T. Oyama, Y. Fujiwara, T. Ohnishi, H. Iwasaki, H. Shinagawa, M. Ariyoshi, K. Mayanagi and K. Morikawa (2002) Crystal structure of the RuvA-RuvB complex. *Mol. Cell* **10**, 671–681.
56. Amiard, S., M. Doudeau, S. Pinte, A. Poulet, C. Lenain, C. Faivre-Moskalenko, D. Angelov, N. Hug, A. Vindigni, P. Bouvet, J. Paoletti, E. Gilson and M.-J. Giraud-Panis (2007) A topological mechanism for TRF2-enhanced strand invasion. *Nat. Struct. Mol. Biol* **14**, 147–154.

Angelov et al., Interstrand Crosslinking Involving Guanine: A New Major UVC Laser-Induced Biphotonic Oxidatively Generated DNA Damage

Figure S1. Denaturing gel electrophoresis of mutated DNA duplexes lacking the 3' guanines A'/B' were submitted to one or several UV laser pulses with a different laser fluence to the same total irradiation dose of 140 mJ/cm^2 and the sequence of the A'/B' mutated DNA dupexe used.

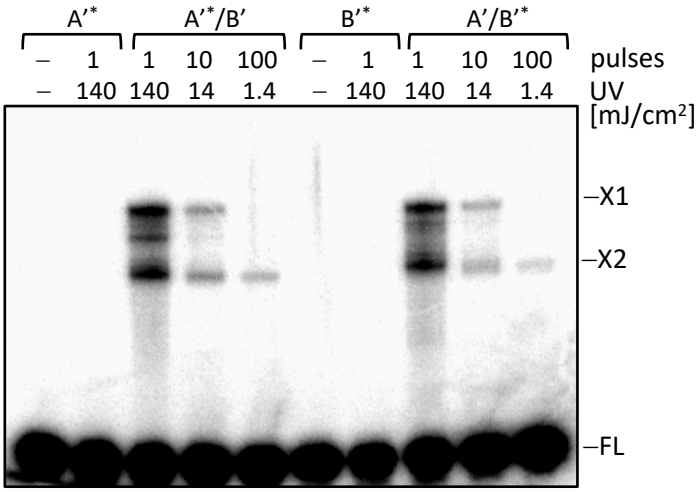

A'/B': 5'–ATATTATACGAATATTTATA–3'
3'–TATAATATGCTTATAAATAT–5'